







Biochemical Study on Bioactive Peptides: Potential Anti-aldose Reductase Targeting Diabetes mellitus

Abel K. Oyebamiji ^{1,*}, Emmanuel T. Akintayo ^{1,2}, Cecilia O. Akintayo ^{1,3}, Halleluyah O. Aworinde⁴, Oluwatobi D. Adekunle ¹, Sunday A. Akintelu ⁵

¹ Industrial Chemistry Programme, Bowen University, Iwo, Osun State, Nigeria; abeloyebamiji@gmail.com (A.K.O.);

² Department of Chemistry, Ekiti State University, Ado-Ekiti, Nigeria; emmanuel.akintayo@bowen.edu.ng (E.T.A.);

³ Department of Chemistry, Federal University, Oye-Ekiti, Ekiti State, Nigeria; cecilia.akintayo@bowen.edu.ng (C.O.A.);

⁴ College of Computing and Communication Studies, Bowen University, Iwo, Nigeria; aworinde.halleluyah@bowen.edu.ng (O.D.A.);

⁵ School of Chemistry and Chemical Engineering, Beijing Institute of Technology, Beijing 100811, China; akintelusundayadewale@gmail.com (S.A.A.);

* Correspondence: abeloyebamiji@gmail.com (A.K.O.); cecilia.akintayo@bowen.edu.ng (C.O.A.);

Scopus Author ID 57189714998

Received: 26.03.2023; Accepted: 2.05.2023; Published: 13.08.2023

Abstract: Diabetes mellitus is a metabolic syndrome that poses a stern threat to global health. The need to stop this menace has attracted the attention of several scientists globally. This work synthesized six peptides, and their anti-aldose reductase activities were investigated using a computational approach to down-regulate diabetes mellitus. All the synthesized compounds yielded well, and all the studied compounds were optimized. All the obtained descriptors from the studied compounds proved to describe the anti-aldose reductase activities of the studied compounds. Also, the non-bonding interactions between the studied peptides and aldose reductase using the docking method were observed, and it was observed that all the compounds under study possess a better ability to inhibit than the referenced drug (Metformin). More so, compound 4 with -8.1kcal/mol proved to have a better ability to inhibit aldose reductase, thereby down-regulate diabetes mellitus than other studied compounds and the referenced drug. The ADMET properties of compound 4 and metformin were examined and reported.

Keywords: aldose reductase; peptides; diabetes mellitus; docking; ADMET.

© 2023 by the authors. This article is an open-access article distributed under the terms and conditions of the Creative Commons Attribution (CC BY) license (<https://creativecommons.org/licenses/by/4.0/>).

1. Introduction

The rise in the blood sugar level in human beings, a metabolic syndrome, has been described as a global challenge [1]. Diabetes mellitus is zed into two forms: type I diabetes mellitus (insulin-reliant) and type II diabetes mellitus (non-insulin reliant). Diabetes has been rated to be third among diseases causing death amidst among men and women, and this has drawn the attention of many researchers globally [2,3]. Many researchers have considered type II of this deadly disease to be chronic and common compared to type I diabetes mellitus [4-6]. The havoc caused by this disease increases, which can be attributed to changes in lifestyle among human beings [7]. Treatment of diabetes mellitus among the human race includes medications, balance diet intake, frequent exercise, and living healthily [8].

The role played by aldose reductase in catalyzing the reduction of several hydrophobic and hydrophilic aldehydes has been described to be crucial in biological systems [9]. It helps in facilitating glucose to diminish to sugar alcohol (Sorbitol) which has been observed by many

researchers to be involved in causing diabetics. According to DeI-Corso *et al.*, 2013, aldose reductase plays an imperative role in the polyol pathway [9], and this has made it to be a vital target receptor, thereby down-regulating diabetic progression [10]. Also, aldose reductase plays serious roles in diseases such as inflammation, cancer, ischemic, etc. [11-14].

Many researchers have reported peptides to have comprehensive antimicrobial actions such as antiendotoxin, anti-diabetic, antiparasitic, anticancer, spermicidal, insecticidal, and antioxidant [15-17]. As reported by Korhonen & Pihlanto, 2006, peptides with biological potentials are definite protein fragments that have a positive impact on human beings [18]; also, it has been observed to have a series of characteristics that make it to be therapeutic and used as anti-diabetic, anticancer and antithrombotic agents [19].

Therefore, this work aims to synthesize six (6) peptides with anti-diabetic activity and observe non-bonding interactions between the studied peptides and aldose reductase with PDB ID: 3g5e [20].

2. Materials and Methods

2.1. General procedures for the synthesis of studied peptides

A series of steps involved in synthesizing the studied peptides were shown in Figure 1 and the steps were loading, coupling, deprotection, solid phase peptide synthesis (SPPS), cleavage, and side chain deprotection.

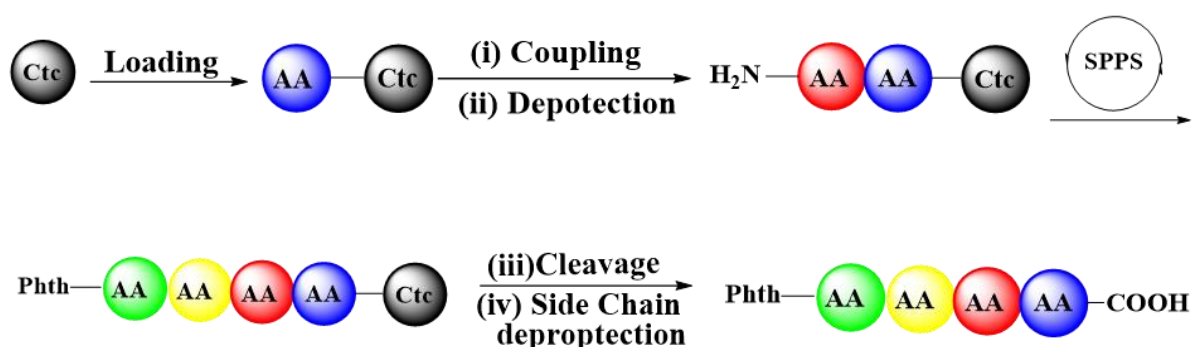


Figure 1. Step-by-step methods used in the synthesis of studied peptides.

2.1.1. Loading of 2-Cl-Trt resin.

Resin (2-chlorotriyl chloride) (1.0 equiv) was weighed and transferred into a peptide synthesis tube. 10mL of 1% DIPEA/DCM was added, and it was allowed to swell for 30 min. After the solvent was drained under vacuum, a solution of the corresponding Fmoc amino acid (1.3 equiv) and DIPEA (6.0 equiv) in DCM was added and shaken for 2.5 hrs. 0.5 mL DIPEA and 1 mL MeOH were added and shaken for 30 minutes. The tube was then drained, rinsed thoroughly with DCM, and dried. The amount of amino acid loaded on the resin was then estimated by Fmoc determination.

2.1.2. Deprotection of Fmoc group.

A solution of 20% piperidine in dried DMF was added to the resin, and it was shaken for 3 x 10 min. The resin was washed with (3x 10 mL) of DMF and (3x 10 mL) of DCM.

2.1.3. Coupling of amino acids.

Corresponding Fmoc or Phth protected amino acid (3.0 equiv) and Oxyma (3.0 equiv) in NMP was cooled under an ice bath for several minutes, DIC (3.3 equiv) was added, and the mixture was thoroughly stirred until a clear solution was obtained. The clear solution was added to the resin and shaken for 2.5 h at room temperature. Then the resin was washed with DMF (2x10 mL), DCM (2x10 mL). All equivalents are calculated based on the theoretical loading of the resin.

2.1.4. Cleavage of 2-Cl-Trt resin.

The dry 2-Cl-Trt resin was treated with a solution of 1% TFA in DCM for 2 hours (2 x 1 hour). The solvents were concentrated in vacuo, and the crude peptide was used for the next step without any purification.

2.1.5. Sidechain deprotection.

The peptide was treated with cocktails containing TFA/ H₂O/TIPS (95:2.5:2.5) for 1 hour. The solvents were evaporated under a vacuum at 30 °C; the crude peptide was precipitated by adding cold diethyl ether. After centrifugation, the supernatant was taken out to give the crude peptide, which was dried under vacuum and purified by column chromatography to obtain a white solid in 85 to 90% yield.

2.1.6. General procedures for the synthesis of peptides 4 and 5

The synthetic pathway for peptides 4 and 5 are shown in Figure 2.

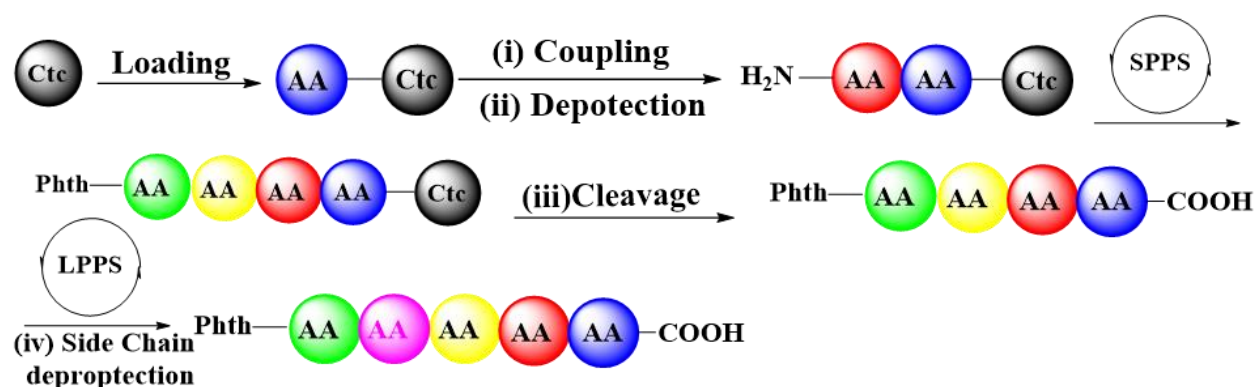


Figure 2. Synthetic pathway for peptides 4 and 5.

2.1.7. Loading of 2-Cl-Trt resin.

Resin (2-chlorotriyl chloride) (1.0 equiv) was weighed and transferred into a peptide synthesis tube. 10mL of 1% DIPEA/DCM was added and allowed to swell for 30 min. After the solvent was drained under vacuum, a solution of the corresponding Fmoc amino acid (1.3 equiv) and DIPEA (6.0 equiv) in DCM was added and shaken for 2.5 hrs. 0.5 mL DIPEA and 1 mL MeOH were added and shaken for 30 minutes. The tube was then drained, rinsed thoroughly with DCM, and dried. The amount of amino acid loaded on the resin was then estimated by Fmoc determination.

2.1.8. Deprotection of Fmoc group.

A solution of 20% piperidine in dried DMF was added to the resin, and it was shaken for 3 x 10 min. The resin was washed with (3x 10 mL) of DMF and (3x 10 mL) of DCM.

2.1.9. Coupling of amino acids.

Corresponding Fmoc or Phth protected amino acid (3.0 equiv) and Oxyma (3.0 equiv) in NMP was cooled under an ice bath for several minutes, DIC (3.3 equiv) was added, and the mixture was thoroughly stirred until a clear solution was obtained. The clear solution was added to the resin and shaken for 2.5 h at room temperature. Then the resin was washed with DMF (2x10 mL), DCM (2x10 mL). All equivalents are calculated based on the theoretical loading of the resin.

2.1.10. Cleavage of 2-Cl-Trt resin.

The dry 2-Cl-Trt resin was treated with a solution of 1% TFA in DCM for 2 hours (2 x 1 hour). The solvents were concentrated in vacuo, and the crude peptide was used for the next step without any purification.

2.1.11. Liquid phase peptide synthesis.

To the crude peptide (1 equiv) obtained from the resin, a solution of L-valine methyl ester hydrochloride (1 equiv) in DMF (10 mL/mmol) was added NMM (3.0 equiv) was added under stirring followed by the addition of (2.2 equiv) HOAt (2.2 equiv) and (2.2 equiv) EDCI. The mixture was stirred at room temperature for 4hrs. Water was added to the reaction mixture and extracted (3x20 mL E.A). The organic layer was washed with 1 M HCl three times, saturated with aqueous NaHCO₃ and brine. The organic layer was dried over anhydrous Na₂SO₄ and concentrated in vacuo to afford the crude sample, which was purified by column chromatography on silica gel with Petroleum ether/ethyl acetate (3/1, v/v) as eluent to give desired peptide 4 and 5 as a white solid (88% yield).

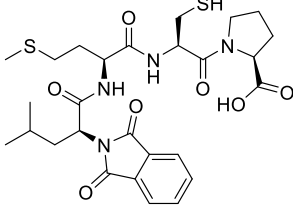
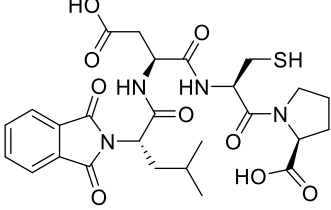
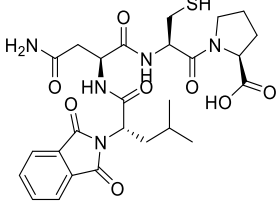
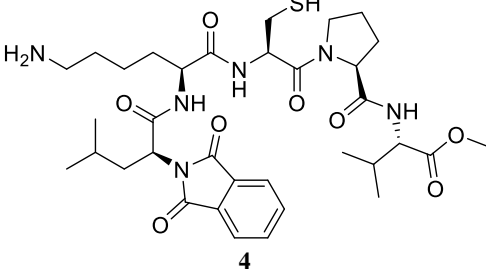
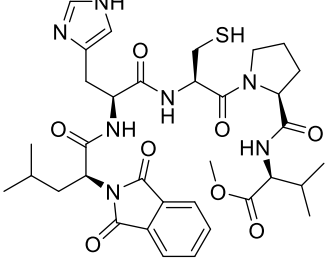
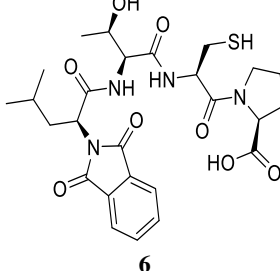
2.1.12. Side chain deprotection.

The peptide was treated with a mixture of cocktails containing TFA/ H₂O/TIPS (95:2.5:2.5) for 1 hour. The solvents were evaporated under a vacuum at 30⁰C; the crude peptide was precipitated by the addition of cold diethyl ether. After centrifugation, the supernatant was taken out to give the crude peptide, which was dried under vacuum and purified by column chromatography to obtain a white solid in 85 to 90% yield.

2.2. *Insilico calculations.*

The synthesized peptide compounds were optimized via the density functional theory method using Spartan 14 software via 6-31G* as a basis set [21, 22]. The density functional theory method used a three-parameter density functional, including Becke's gradient exchange correction [23, 24] and the Lee, Yang, Parr correlation functional. The IUPAC names of the studied peptides are listed in Table 1.

Table 1. 2D Schematic structure of the studied peptides.

 <p>1 ((S)-2-(1,3-dioxoisindolin-2-yl)-4-methylpentanoyl)-L-methionyl-L-cysteinyl-L-proline</p>	 <p>2 ((S)-2-(1,3-dioxoisindolin-2-yl)-4-methylpentanoyl)-L-aspartyl-L-cysteinyl-L-proline</p>	 <p>3 ((S)-2-(1,3-dioxoisindolin-2-yl)-4-methylpentanoyl)-L-asparaginyl-L-cysteinyl-L-proline</p>
 <p>4 Methyl ((S)-2-(1,3-dioxoisindolin-2-yl)-4-methylpentanoyl)-L-lysyl-L-cysteinyl-L-prolyl-L-valinate</p>	 <p>5 Methyl ((S)-2-(1,3-Dioxoisindolin-2-yl)-4-Methylpentanoyl)-L-Histidyl-L-Cysteinyl-L-Prolyl-L-Valinate</p>	 <p>6 ((S)-2-(1,3-dioxoisindolin-2-yl)-4-methylpentanoyl)-L-threonyl-L-cysteinyl-L-proline</p>

2.2.1. Molecular docking calculations.

The optimized peptide compounds were prepared by converting the optimized compounds to .pdb format and further subjected to auto dock tool software to convert them to .pdbqt. Also, a series of factors were considered before choosing the target from the protein database, and the factors were resolution (1.80 Å), R-value free (0.183), R-value work (0.144), and R-Value Observed (0.146), respectively. The downloaded aldose reductase from the protein data bank was treated by removing water molecules and any small molecules downloaded with the target receptor using pymol software and further subjected to auto dock tool software to locate the active site in the aldose reductase (PDB ID: 3g5e) and converted it to the acceptable format (.pdbqt) by auto dock vina for docking calculations. The details for the active site in the studied receptor were as follows: center (X = 14.243, Y = 0.074, Z = 23.805) and size (X = 64, Y = 52, Z = 58), and spacing was set to be 1.00Å (figure 3).

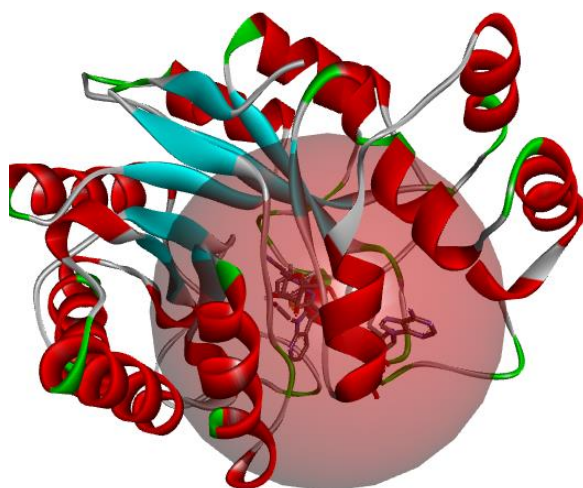


Figure 3. 3-D structure of Human aldose reductase (3g5e) with identified active site.

3. Results and Discussion

The synthesized compounds yielded the followings:

3.1.1. ((S)-2-(1,3-dioxisoindolin-2-yl)-4-methylpentanoyl)-L-methionyl-L-cysteinyl-L-proline (1).

^1H NMR (400 MHz, DMSO) δ 8.26 (dd, $J = 18.8, 7.8$ Hz, 2H), 7.93 – 7.83 (m, 4H), 4.74 (dd, $J = 11.4, 4.4$ Hz, 1H), 4.56 (m, $J = 14.0, 6.8$ Hz, 1H), 4.42 – 4.34 (m, 2H), 3.70 – 3.60 (m, 2H), 2.85 – 2.75 (m, 1H), 2.62 (m, $J = 13.5, 9.1, 6.8$ Hz, 1H), 2.43 – 2.27 (m, 3H), 2.15 (m, $J = 12.0, 9.2, 6.1$ Hz, 1H), 2.10 – 1.99 (m, 1H), 1.96 (s, 3H), 1.94 – 1.78 (m, 5H), 1.71 (m, $J = 9.3, 4.5$ Hz, 1H), 1.39 – 1.30 (m, 1H), 0.85 (m, $J = 11.3, 6.6$ Hz, 6H) (Figure 4).

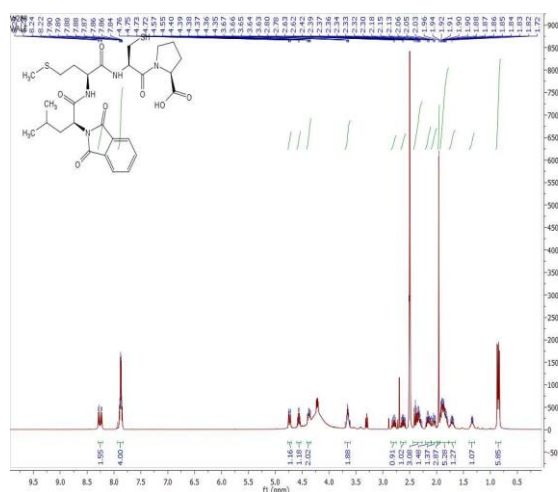


Figure 4. Proton NMR for compound 1.

3.1.2. ((S)-2-(1,3-dioxisoindolin-2-yl)-4-methylpentanoyl)-L-aspartyl-L-cysteinyl-L-proline (2).

^1H NMR (400 MHz, DMSO) δ 8.40 (d, $J = 7.9$ Hz, 1H), 8.04 (d, $J = 7.8$ Hz, 1H), 7.91 – 7.84 (m, 4H), 4.75 (dd, $J = 11.6, 4.3$ Hz, 1H), 4.57 (m, $J = 7.1, 4.6$ Hz, 2H), 4.23 (dd, $J = 8.7, 4.4$ Hz, 1H), 3.62 (t, $J = 6.1$ Hz, 2H), 2.84 – 2.72 (m, 1H), 2.63 (m, $J = 13.6, 12.7, 6.7$ Hz, 2H), 2.35 (mf, $J = 17.4, 15.3, 7.9$ Hz, 2H), 2.20 – 2.07 (m, 2H), 1.94 – 1.79 (m, 4H), 1.35 (d, $J = 6.4$ Hz, 1H), 1.29 – 1.20 (m, 1H), 0.85 (t, $J = 7.1$ Hz, 6H) (Figure 5).

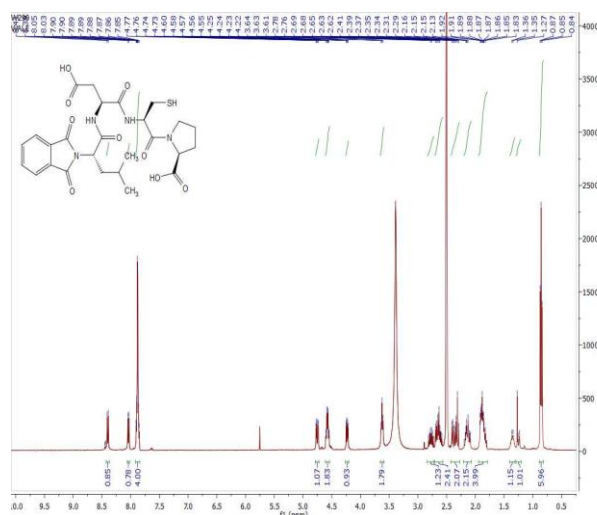


Figure 5. Proton NMR for compound 2.

3.1.3. ((S)-2-(1,3-dioxisoindolin-2-yl)-4-methylpentanoyl)-L-asparaginyl-L-cysteinyl-L-proline (3).

^1H NMR (400 MHz, DMSO) δ 8.38 (d, $J = 7.8$ Hz, 1H), 8.30 (d, $J = 7.8$ Hz, 1H), 8.12 (d, $J = 8.0$ Hz, 1H), 7.97 (d, $J = 7.9$ Hz, 1H), 7.94 – 7.81 (m, 1H), 7.21 (d, $J = 12.2$ Hz, 1H), 6.83 (s, 1H), 4.75 (M, 1H), 4.56 (M, 1H), 4.31 – 4.15 (m, 1H), 3.07 (dd, $J = 14.0, 5.7$ Hz, 1H), 2.89 – 2.70 (m, 1H), 2.70 – 2.58 (m, 1H), 2.39 – 2.22 (m, 1H), 2.14 (M, 1H), 1.95 – 1.77 (m, 1H), 1.35 (s, 1H), 1.27 – 1.07 (m, 1H), 0.85 (t, $J = 6.7$ Hz, 1H) (Figure 6).

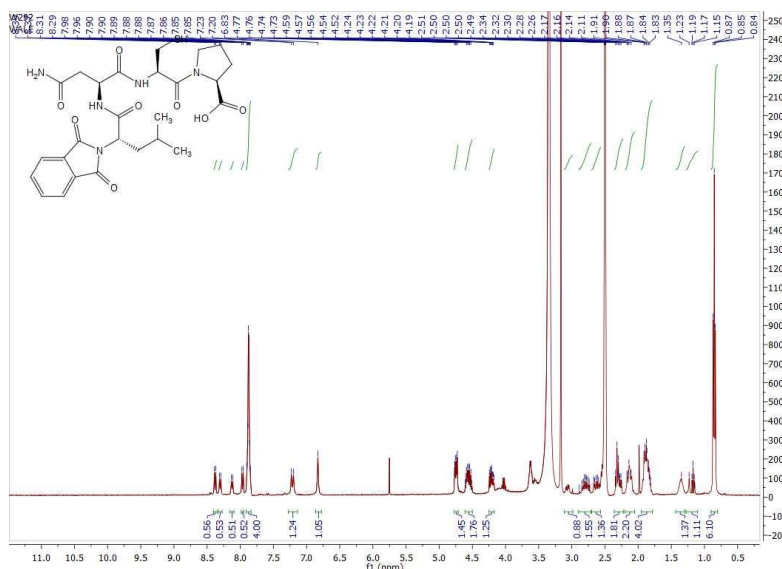


Figure 6. Proton NMR for compound 3.

3.1.4. Methyl ((S)-2-(1,3-dioxisoindolin-2-yl)-4-methylpentanoyl)-L-lysyl-L-cysteinyl-L-prolyl-L-valinate (4).

^1H NMR (400 MHz, DMSO) δ 8.25 (d, $J = 8.0$ Hz, 1H), 8.18 (d, $J = 7.3$ Hz, 1H), 8.12 (d, $J = 8.2$ Hz, 1H), 7.92 – 7.81 (m, 4H), 4.79 – 4.68 (m, 1H), 4.62 – 4.51 (m, 1H), 4.48 – 4.38 (m, 1H), 4.34 – 4.22 (m, 1H), 4.19 – 4.11 (m, 1H), 3.61 (s, 3H), 2.83 – 2.55 (m, 5H), 2.14 – 1.98 (m, 3H), 1.95 – 1.75 (m, 4H), 1.65 – 1.54 (m, 1H), 1.53 – 1.38 (m, 3H), 1.38 – 1.30 (m, 1H), 1.30 – 1.12 (m, 3H), 0.94 – 0.78 (m, 12H) (Figure 7).

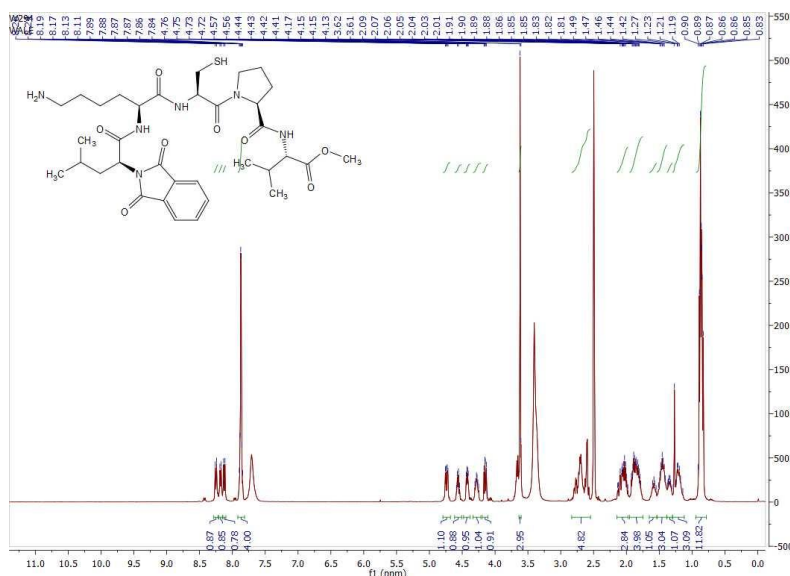


Figure 7. Proton NMR for compound 4.

3.1.5. Methyl ((S)-2-(1,3-Dioxoisindolin-2-Yl)-4-Methylpentanoyl)-L-Histidyl-L-Cysteinyl-L-Prolyl-L-Valinate (5).

^1H NMR (400 MHz, DMSO) δ 8.89 (d, $J = 8.0$ Hz, 1H), 8.50 – 8.34 (m, 2H), 8.21 (d, $J = 7.3$ Hz, 1H), 8.11 (dd, $J = 23.6, 8.2$ Hz, 1H), 7.87 (d, $J = 1.5$ Hz, 4H), 7.33 (d, $J = 4.6$ Hz, 1H), 7.07 (d, $J = 16.4$ Hz, 1H), 4.79 – 4.70 (m, 1H), 4.69 – 4.56 (m, 2H), 4.46 – 4.38 (m, 1H), 4.19 – 4.08 (m, 1H), 3.62 (s, 3H), 3.09 – 2.98 (m, 2H), 2.92 – 2.74 (m, 2H), 2.73 – 2.55 (m, 2H), 2.10 – 1.93 (m, 3H), 1.93 – 1.78 (m, 4H), 1.36 – 1.20 (m, 2H), 0.93 – 0.77 (m, 12H) (Figure 8).

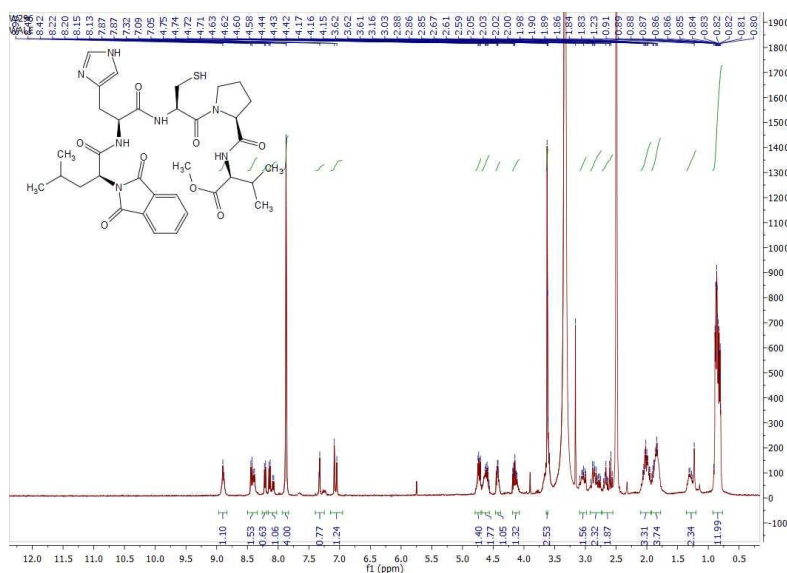


Figure 8. Proton NMR for compound 5.

3.1.6. ((S)-2-(1,3-dioxoisindolin-2-yl)-4-methylpentanoyl)-L-threonyl-L-cysteinyl-L-proline (6).

^1H NMR (400 MHz, DMSO) δ 8.53 (d, $J = 7.7$ Hz, 1H), 7.91 – 7.83 (m, 4H), 7.78 (d, $J = 8.7$ Hz, 1H), 4.72 (dd, $J = 11.6, 4.2$ Hz, 1H), 4.63 (dd, $J = 12.7, 5.4$ Hz, 1H), 4.50 (dd, $J = 8.2, 3.0$ Hz, 1H), 4.20 – 4.09 (m, 2H), 2.80 – 2.63 (m, 2H), 2.21 – 2.01 (m, 3H), 1.96 – 1.82 (m, 4H), 1.34 (d, $J = 6.5$ Hz, 1H), 1.23 (d, $J = 5.1$ Hz, 1H), 1.05 (d, $J = 6.3$ Hz, 3H), 0.88 – 0.82 (m, 6H) (Figure 9).

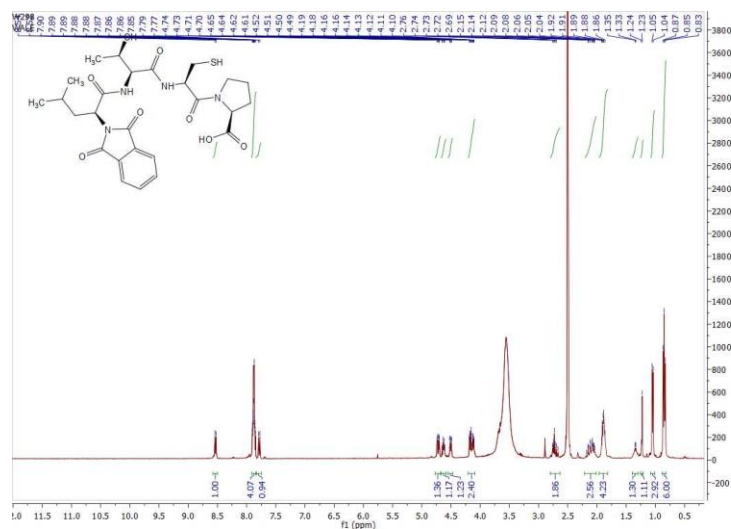


Figure 9. Proton NMR for compound 6.

3.2. Calculated descriptors obtained from the studied compounds.

The optimized compounds brought about the series of descriptors (highest occupied molecular orbital energy (E_{HOMO}), lowest unoccupied molecular orbital energy (E_{LUMO}), dipole moment (DM), molecular weight (MW), ovality, polar surface area (PSA), polarizability, hydrogen bond donor (HBD), hydrogen bond acceptor (HBA) and lipophilicity (LogP)). According to Oyebamiji *et al.*, 2021, the ability of a molecular compound to release electron to the neighboring compound reveal the role of E_{HOMO} , and as shown in Table 2, it was observed that compound 1 is expected to interact and inhibit better than other studied compounds [23]. Also, the capacity of any compound to accept an electron from the neighboring compound reveals the role of E_{LUMO} ; thus, compound 4 is expected to inhibit aldose reductase better than other studied compounds.

Furthermore, the strength of any compound to dissolve into a non-aqueous solution revealed the role played by Log P in drug design and development [24]. More so, an arbitrary higher Log P value than 5 for any compound indicates problematic oral absorptivity of the studied compounds [25]; thus, all the studied compounds proved to have the ability to act as a drug. Other descriptors were reported in Table 2.

Table 2. Calculated descriptors obtained from compounds from synthesized Peptides.

	E_{HOMO}	E_{LUMO}	DM	MW	PSA	OVALITY	POL	HBD	HBA	Log P
1	-5.92	-2.35	10.56	592.73	113.22	1.82	86.70	4	12	-0.40
2	-6.49	-2.34	10.22	576.62	143.57	1.77	84.18	5	12	-1.69
3	-6.46	-2.33	8.32	575.64	153.32	1.79	84.53	5	13	-2.34
4	-6.06	-2.38	12.35	702.87	155.72	1.94	97.65	4	14	-0.71
5	-6.04	-2.32	8.60	711.84	148.59	1.92	97.08	4	14	-1.64
6	-6.45	-2.36	12.62	562.64	123.40	1.76	83.93	5	12	-1.45

Note: E_{HOMO} : Highest occupied molecular orbital energy; E_{LUMO} : lowest unoccupied molecular orbital energy; DM: dipole moment; MW: molecular weight; PSA: Polar surface area; POL: Polarizability; HBD: hydrogen bond donor; HBA: Hydrogen bond acceptor; Log P: Lipophilicity

3.2. Molecular docking calculations.

Molecular docking calculations on synthesized peptides against aldose reductase (PDB ID: 3g5e) were investigated to observe non-bonding interactions and binding affinities between the studied peptide- aldose reductase complexes. The calculated binding affinity for compounds 1 – 6 was -6.4 kcal/mol, -6.4 kcal/mol, -6.6 kcal/mol, -8.1 kcal/mol, -7.2 kcal/mol, and -6.5 kcal/mol, respectively (Table 3). According to Oyebamiji *et al.* 2020, a lower binding affinity value for any molecular compound indicates its better tendency to inhibit better [26]; thus, compound 4 with -8.1 kcal/mol proved to possess a better ability to inhibit than other studied compounds as well as the referenced drug. The ability of compound 4 to receive electrons from aldose reductase, as reported in Table 2 was observed to enhance its ability to interact well and to inhibit aldose reductase than other studied compounds as well as Metformin (Referenced Drug) (Figure 10).

Also, the combination of amino acid residues as well as the types of non-bonding interaction involved in the interaction between Methyl ((S)-2-(1,3-dioxisoindolin-2-yl)-4-methylpentanoyl)-L-lysyl-L-cysteinyl-L-prolyl-L-valinate (4) and aldose reductase (PDB ID: 3g5e) complex was observed to contribute to greater stability of compound 4 in the active site of the studied receptor which thereby led to its highest binding affinity among other studied compounds.

The residue involved in the interaction were Trp20, Trp219, Cys298, Trp111, Trp79, Phe122, Leu300, Leu124 for compound 1; Phe273, Phe276, Arg40, Arg3, Gly38 for compound 2; Arg255, Ile196, Gln200, Ser282 for compound 3; Tyr48, Val47, Trp79, His110, Trp111, Leu300, Cys303, Cys298, Gln49, Trp20 for compound 4; Leu124, Phe121, Phe122, Leu300, Gln49, Glu120, Cys298, Trp111, Trp219, Trp20 for compound 5 and Glu193, Ser282, Lys194 for compound 6.

Table 3. Calculated binding affinity, types of interaction, and amino acid residues involved in the interaction.

	Binding Affinity (kcal/mol)	Residues involved in the interactions	Types of Non-bonding interaction involved
1	-6.4	Trp20, Trp219, Cys298, Trp111, Trp79, Phe122, Leu300, Leu124	Conventional Hydrogen Bond, Carbon Hydrogen bond, Unfavourable Donor-Donor, Pi-Anion, Pi-Alkyl
2	-6.4	Phe273, Phe276, Arg40, Arg3, Gly38	Conventional Hydrogen Bond, Carbon Hydrogen bond, Unfavourable Acceptor-Acceptor, Pi-Anion, Pi-Alkyl
3	-6.6	Arg255, Ile196, Gln200, Ser282	Conventional Hydrogen Bond, Carbon Hydrogen bond, Pi-Pi Stacked, Pi-Alkyl
4	-8.1	Tyr48, Val47, Trp79, His110, Trp111, Leu300, Cys303, Cys298, Gln49, Trp20	Conventional Hydrogen Bond, Pi-Alkyl
5	-7.2	Leu124, Phe121, Phe122, Leu300, Gln49, Glu120, Cys298, Trp111, Trp219, Trp20	Conventional Hydrogen Bond, Carbon Hydrogen bond, Pi-Anion, Pi-Pi T-Shaped, Pi-Alkyl
6	-6.5	Glu193, Ser282, Lys194	Conventional Hydrogen Bond, Carbon Hydrogen bond, Pi-Sigma, Alkyl
Metformin	-6.0	-	-

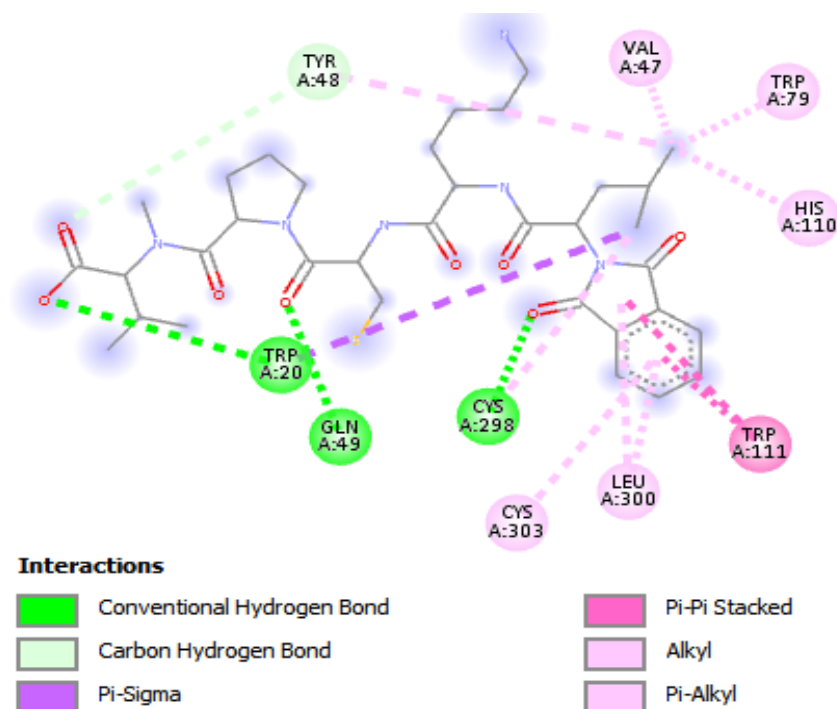


Figure 10. 2D structure for compound 4 against aldose reductase (PDB ID: 3g5e).

3.3. Predicted ADME properties.

The physicochemical properties, lipophilicity, water solubility, pharmacokinetics, drug-likeness, and medicinal chemistry of the selected compounds with higher binding affinity were investigated using online ADMETSAR software. It was observed that the ADMET property for the selected compound was similar to the ADMET properties obtained for metformin (Standard). The predicted blood-brain barrier, Caco-2 Permeability, and Human intestinal absorption value for compound 14 were closer to the calculated value for metformin. As shown in Table 4, it was observed that compound 4 and metformin were non-inhibitor of

CYP450 1A2, CYP450 2D6, CYP450 2C19, and metformin was observed not to inhibit CYP450 3A4 but compound 4 inhibited CYP450 3A4. Also, compound 4 and metformin were observed to inhibit CYP450 2C9. Both selected compounds were non-carcinogens, and they were not readily biodegradable.

Table 4. ADMET investigation on Selected compounds.

Mode	Compound 4		Metformin	
	Result	Probability	Result	Probability
Blood-Brain Barrier	BBB-	0.7977	BBB-	0.7895
Human Intestinal Absorption	HIA+	0.9577	HIA+	0.9651
Caco-2 Permeability	Caco2-	0.5653	Caco2-	0.5726
P-glycoprotein Substrate	Non-substrate	0.6280	Non-substrate	0.5683
P-glycoprotein Inhibitor	Non-inhibitor	0.7827	Non-inhibitor	0.8341
	Non-inhibitor	0.9304	Non-inhibitor	0.9002
Renal Organic Cation Transporter	Non-inhibitor	0.9481	Non-inhibitor	0.9223
Subcellular localization	Mitochondria	0.6466	Mitochondria	0.6265
CYP450 2C9 Substrate	Non-substrate	0.5668	Non-substrate	0.6119
CYP450 2D6 Substrate	Non-substrate	0.8171	Non-substrate	0.8114
CYP450 3A4 Substrate	Substrate	0.5087	Substrate	0.5063
CYP450 1A2 Inhibitor	Non-inhibitor	0.6687	Non-inhibitor	0.6061
CYP450 2C9 Inhibitor	Inhibitor	0.5234	Inhibitor	0.5501
CYP450 2D6 Inhibitor	Non-inhibitor	0.8407	Non-inhibitor	0.8559
CYP450 2C19 Inhibitor	Non-inhibitor	0.5223	Non-inhibitor	0.5338
CYP450 3A4 Inhibitor	Inhibitor	0.6075	Non-inhibitor	0.7272
CYP Inhibitory Promiscuity	High CYP Inhibitory Promiscuity	0.7338	High CYP Inhibitory Promiscuity	0.6369
Human Ether-a-go-go-Related Gene Inhibition	Weak inhibitor	0.9923	Weak inhibitor	0.9973
	Non-inhibitor	0.5838	Non-inhibitor	0.5526
AMES Toxicity	Non AMES toxic	0.5139	Non AMES toxic	0.6247
Carcinogens	Non-carcinogens	0.8055	Non-carcinogens	0.8039
Fish Toxicity	High FHMT	0.9864	High FHMT	0.9947
Tetrahymena Pyriformis Toxicity	High TPT	0.9904	High TPT	0.9941
Honey Bee Toxicity	Low HBT	0.7298	Low HBT	0.7545
Biodegradation	Not ready biodegradable	0.9789	Not ready biodegradable	0.9944

4. Conclusions

The menace caused by diabetes mellitus amidst males and females calls for urgent attention. The dreadedness of this disease has caused several scientists to keep working and searching for a lasting solution; therefore, six (6) peptides were synthesized, and their biological interactions were studied using *in silico* approach. The synthesized peptides were observed to be appropriate, and all the studied compounds proved to be biologically active. It was observed that compound 4 proved to possess a better ability to inhibit aldose reductase than other studied compounds and Metformin (Reference drug), thereby down-regulating diabetes mellitus using *in silico* approach. Also, the ADMET properties of compound 4 and metformin were investigated and reported. Our findings may open the door for designing and developing a library of efficient peptide-based drug-like compounds as potential anti-diabetic agents.

Funding

We are grateful to Bowen University Research Grant Programme for the grant (Grant No: BURG/2023/009).

Acknowledgments

We are grateful to the Industrial Chemistry Programme, Bowen University, for the computational resources and to Mrs E.T. Oyebamiji, as well as Miss Priscilla F. Oyebamiji, for the assistance in the course of this study.

Conflicts of Interest

The authors declare no conflict of interest.

References

1. Ghaffari, M.; Razi, S.; Zalpoor, H.; Nabi-Afjadi, M.; Mohebichamkhorami, F.; Zali, H. Association of MicroRNA-146a with Type 1 and 2 Diabetes and their Related Complications. *Journal of Diabetes Research* **2023**, *2023*, <https://doi.org/10.1155/2023/2587104>.
2. Oyebamiji, A.K.; Soetan, E.A.; Akintelu, S.A.; Ayeleso, A.O.; Mukwevho, E. Alpha-glucosidase activity of phytochemicals from *Phyllanthus amarus* leaves via in-silico approaches. *Pharmacological Research - Modern Chinese Medicine* **2022**, *2*, <https://doi.org/10.1016/j.prmcm.2022.100054>.
3. Liu, S.; Zeng, M.; Wan, W.; Huang, M.; Li, X.; Xie, Z.; Wang, S.; Cai, Y. The Health-Promoting Effects and the Mechanism of Intermittent Fasting. *Journal of Diabetes Research* **2023**, *2023*, <https://doi.org/10.1155/2023/4038546>.
4. Wang, J.; Wu, T.; Fang, L.; Liu, C.; Liu, X.; Li, H.; Shi, J.; Li, M.; Min, W. Anti-diabetic effect by walnut (*Juglans mandshurica* Maxim.)-derived peptide LPLLR through inhibiting α -glucosidase and α -amylase, and alleviating insulin resistance of hepatic HepG2 cells. *Journal of Functional Foods* **2020**, *69*, <https://doi.org/10.1016/j.jff.2020.103944>.
5. Liu, J.; Fu, H.; Kang, F.; Ning, G.; Ni, Q.; Wang, W.; Wang, Q. β -Cell glucokinase expression was increased in type 2 diabetes subjects with better glycemic control. *Journal of Diabetes* **2023**, *1-10*, <https://doi.org/10.1111/1753-0407.13380>.
6. Soltaninejad, H.; Zare-Zardini, H.; Ordooei, M.; Ghelmani, Y.; Ghadiri-Anari, A.; Mojahedi, S.; Hamidieh, A.A. Antimicrobial Peptides from Amphibian Innate Immune System as Potent Antidiabetic Agents: A Literature Review and Bioinformatics Analysis. *Journal of Diabetes Research* **2021**, *2021*, <https://doi.org/10.1155/2021/2894722>.
7. Ordooei, M.; Shojaaddiny, A.; Hoseinipoor, S.; Soleimanizad, R.; Miroliai, M.; Zardini, H. Effect of Vitamin D on HbA1c levels of children and adolescents with diabetes mellitus type 1. *Minerva pediatrica* **2014**, *69*, 391-395, <https://doi.org/10.23736/S0026-4946.16.04145-1>.
8. LeRoith, D.; Biessels, G.J.; Braithwaite, S.S.; Casanueva, F.F.; Draznin, B.; Halter, J.B.; Hirsch, I.B.; McDonnell, M.E.; Molitch, M.E.; Murad, M.H.; Sinclair, A.J. Treatment of Diabetes in Older Adults: An Endocrine Society* Clinical Practice Guideline. *The Journal of clinical endocrinology and metabolism* **2019**, *104*, 1520-1574, <https://doi.org/10.1210/je.2019-00198>.
9. Del-Corso, A.; Balestri, F.; Di Bugno, E.; Moschini, R.; Cappiello, M.; Sartini, S.; La-Motta, C.; Da-Settimo, F.; Mura, U. A New Approach to Control the Enigmatic Activity of Aldose Reductase. *PLOS ONE* **2013**, *8*, <https://doi.org/10.1371/journal.pone.0074076>.
10. Suzen, S.; Buyukbingol, E. Recent studies of aldose reductase enzyme inhibition for diabetic complications. *Curr Med Chem* **2003**, *10*, 1329-1352, <https://doi.org/10.2174/0929867033457377>.
11. Alexiou, P.; Pegklidou, K.; Chatzopoulou, M.; Nicolaou, I.; Demopoulos, J.V. Aldose Reductase Enzyme and its Implication to Major Health Problems of the 21st Century. *Current Medicinal Chemistry* **2009**, *16*, 734-752, <https://doi.org/10.2174/092986709787458362>.
12. Bresson, E.; Lacroix-Péppin, N.; Boucher-Kovalik, S.; Chapdelaine, P.; Fortier, MA. The prostaglandin F synthase activity of the human aldose reductase AKR1B1 brings new lenses to look at pathologic conditions. *Front Pharmacol.* **2012**, *3*, <https://doi.org/10.3389/fphar.2012.00098>.
13. Pandey, S.; Srivastava, S.K.; Ramana, K.V. A potential therapeutic role for aldose reductase inhibitors in the treatment of endotoxin-related inflammatory diseases. *Expert Opinion on Investigational Drugs* **2012**, *21*, 329-339, <https://doi.org/10.1517/13543784.2012.656198>.
14. Laffin, B.; Petrash, M. Expression of the Aldo-Ketoreductases AKR1B1 and AKR1B10 in Human Cancers. *Frontiers in Pharmacology* **2012**, *3*, <https://doi.org/10.3389/fphar.2012.00104>.
15. Oyebamiji, A.K.; Soetan, E.A.; Akintelu, S.A.; Ayeleso, A.O.; Mukwevho, E. Alpha-glucosidase activity of phytochemicals from *Phyllanthus amarus* leaves via in-silico approaches. *Pharmacological Research - Modern Chinese Medicine* **2022**, *2*, 100054, <https://doi.org/10.1016/j.prmcm.2022.100054>.
16. Khani, S.; Seyedjavadi, S.S.; Zare-Zardini, H.; Hosseini, H.M.; Goudarzi, M.; Khatami, S.; Amani, J.; Imani Fooladi, A.A.; Razzaghi-Abyaneh, M. Isolation and functional characterization of an antifungal hydrophilic

- peptide, Skh-AMP1, derived from *Satureja khuzistanica* leaves. *Phytochemistry* **2019**, *164*, 136-143, <https://doi.org/10.1016/j.phytochem.2019.05.011>.
17. Seyedjavadi, S.S.; Khani, S.; Eslamifar, A.; Ajdary, S.; Goudarzi, M.; Halabian, R.; Akbari, R.; Zare-Zardini, H.; Imani Fooladi, A.A.; Amani, J.; Razzaghi-Abyaneh, M. The Antifungal Peptide MCh-AMP1 Derived From *Matricaria chamomilla* Inhibits *Candida albicans* Growth via Inducing ROS Generation and Altering Fungal Cell Membrane Permeability. *Frontiers in Microbiology* **2020**, *10*, <https://doi.org/10.3389/fmicb.2019.03150>.
 18. Korhonen, H.; Pihlanto, A. Bioactive peptides: Production and functionality. *International Dairy Journal* **2006**, *16*, 945-960, <https://doi.org/10.1016/j.idairyj.2005.10.012>.
 19. Yan, J.; Zhao, J.; Yang, R.; Zhao, W. Bioactive peptides with anti-diabetic properties: a review. *International Journal of Food Science & Technology* **2019**, *54*, 1909-1919, <https://doi.org/10.1111/ijfs.14090>.
 20. Van Zandt, M.C.; Doan, B.; Sawicki, D.R.; Sredy, J.; Podjarny, A.D. Discovery of [3-(4,5,7-trifluorobenzothiazol-2-ylmethyl)-pyrrolo[2,3-b]pyridin-1-yl]acetic acids as highly potent and selective inhibitors of aldose reductase for treatment of chronic diabetic complications. *Bioorganic & medicinal chemistry letters* **2009**, *19*, 2006-2008, <https://doi.org/10.1016/j.bmcl.2009.02.037>.
 21. Oyebamiji, A.K.; Abdulsalami, I.O.; Semire, B. Dataset on Insilico approaches for 3,4-dihydropyrimidin-2(1H)-one urea derivatives as efficient *Staphylococcus aureus* inhibitor. *Data in Brief* **2020**, *32*, <https://doi.org/10.1016/j.dib.2020.106195>.
 22. Adegoke, R.O.; Oyebamiji, A.K.; Semire, B. Dataset on the DFT-QSAR, and docking approaches for anticancer activities of 1, 2, 3-triazole-pyrimidine derivatives against human esophageal carcinoma (EC-109). *Data Brief* **2020**, *31*, <https://doi.org/10.1016/j.dib.2020.105963>.
 23. Oyebamiji, A.K.; Fadare, O.A.; Akintelu, S.A.; Semire, B. Biological Studies on Anthra[1,9-cd]pyrazol-6(2D)-one Analogues as Anti-vascular Endothelial Growth Factor Via In silico Mechanisms. *Chemistry Africa* **2021**, *4*, 955-963, <https://doi.org/10.1007/s42250-021-00276-2>.
 24. Oyebamiji, A.K.; Semire, B. In-Silico Study on Anti-bacteria and Anti-fungal Activities of 3,4-Dihydropyrimidin-2(1H)-One Urea Derivatives. *Chemistry Africa* **2021**, *4*, 149-159, <https://doi.org/10.1007/s42250-020-00202-y>.
 25. Meanwell, N.A. Synopsis of some recent tactical application of bioisosteres in drug design. *Journal of medicinal chemistry* **2011**, *54*, 2529-2591, <https://doi.org/10.1021/jm1013693>.
 26. Oyebamiji, A.; Akintelu, S.A.; Mutiu, O.; Adeosun, I.; Kaka, M.; Olotu, T.; Soetan, A.; Adelowo, J.; Semire, B. In-Silico Study on Anti-cancer Activity of Selected Alkaloids from *Catharanthus roseus*. *Trop J Nat Prod Res.* **2021**, *5*, 1315-1322, <https://doi.org/10.26538/tjnpr/v5i7.25>.